

Communication

Stable and inert Mn(II)-based and pH responsive contrast agents

Richárd Botár, Enikő Molnár, György Trencsényi, János Kiss, Ferenc K. Kalman, and Gyula Tircso

J. Am. Chem. Soc., **Just Accepted Manuscript** • Publication Date (Web): 13 Jan 2020

Downloaded from pubs.acs.org on January 13, 2020

Just Accepted

“Just Accepted” manuscripts have been peer-reviewed and accepted for publication. They are posted online prior to technical editing, formatting for publication and author proofing. The American Chemical Society provides “Just Accepted” as a service to the research community to expedite the dissemination of scientific material as soon as possible after acceptance. “Just Accepted” manuscripts appear in full in PDF format accompanied by an HTML abstract. “Just Accepted” manuscripts have been fully peer reviewed, but should not be considered the official version of record. They are citable by the Digital Object Identifier (DOI®). “Just Accepted” is an optional service offered to authors. Therefore, the “Just Accepted” Web site may not include all articles that will be published in the journal. After a manuscript is technically edited and formatted, it will be removed from the “Just Accepted” Web site and published as an ASAP article. Note that technical editing may introduce minor changes to the manuscript text and/or graphics which could affect content, and all legal disclaimers and ethical guidelines that apply to the journal pertain. ACS cannot be held responsible for errors or consequences arising from the use of information contained in these “Just Accepted” manuscripts.

Stable and inert Mn(II)-based and pH responsive contrast agents

Richárd Botár,[†] Enikő Molnár,[†] György Trencsényi,[§] János Kiss,^{§,‡} Ferenc K. Kálmán^{†*} and Gyula Tircsó^{†*}

[†] Department of Physical Chemistry, University of Debrecen, H-4032 Debrecen (Hungary)

[§] Division of Nuclear Medicine, Department of Medical Imaging, Faculty of Medicine, University of Debrecen, H-4032 Debrecen (Hungary)

[‡] Mediso Ltd., H-4032 Debrecen (Hungary)

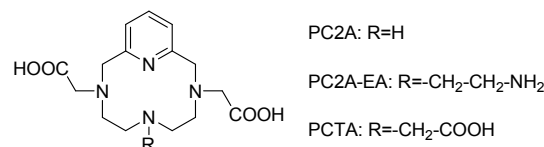
Supporting Information Placeholder

ABSTRACT: Smart/intelligent contrast agent candidates for MRI based on Mn(II) ion are rare as it usually forms labile complexes with polyaminocarboxylate type ligands. Here, we report the first example of a Mn(II) complex that can be activated by changing the pH of its local environment. The PC2A-EA ligand with an ethylamine pendant arm was found to form thermodynamically stable ($pMn=9.27$) and kinetically inert complex with Mn(II) respect to *trans*-chelation with metal ion like Cu(II). The [MnH(PCA2-EA)] complex display relatively slow water exchange rate ($(4.0 \pm 0.2) \times 10^7 \text{ s}^{-1}$), but the pH-dependent coordination of the ethylamine moiety occurs in the pH range of 6-8 enabling the complex to exhibit pH-sensitive relaxivity in the biologically relevant pH range.

Magnetic resonance imaging (MRI) is a non-invasive imaging modality that can generate high resolution images of soft tissues. A large percentage of MR exams use a gadolinium-based contrast agent to enhance contrast between normal and diseased tissues. Newer generation agents that can report specific biomarkers or biochemical processes associated with certain diseases have also been developed.¹⁻³ These responsive compounds are frequently called smart (SCAs) or intelligent CAs. A considerable amount of research effort has been invested into the development of SCAs over the past decades yielding SCA candidates (mostly Gd(III) based compounds) capable of reporting changes in pH,⁴⁻⁶ redox state,⁷⁻⁹ temperature,¹⁰⁻¹² enzyme activity,¹³⁻¹⁵ levels of certain metal ions (Ca^{2+} , Zn^{2+} or Cu^{2+}),^{16,17} O_2 saturation¹⁸⁻²⁰ etc. Most of these agents are based on an established ligand design (i.e. DOTA) that is known to form kinetically inert complexes with Gd(III). However, this does not necessarily mean that the modified complexes would retain the inertness of the parent complex ([Gd(DOTA)]).^{16,21} In the light of nephrogenic systemic fibrosis (NSF), a devastating disease associated with the toxicity of the free Gd(III) produced *in vivo* as a result of the decomplexation of CAs^{22,23} there is a definite need to improve the dissociation kinetics parameters of Gd(III) based CAs and SCAs. On the other hand, finding a plausible alternative to Gd(III)-based CAs has received considerable attention in the past decade. The most promising candidates are complexes of the essential Mn(II) ion because it has acceptable relaxation enhancement properties and its homeostasis and transport in living systems guarantees very efficient elimination form the living systems as it was observed for the [Mn(PyC3A)] chelate recently.²⁴⁻²⁶ However, Mn(II) complexes are in general labile, and only a few examples of inert Mn(II)

complexes are known.²⁷⁻³⁰ The release of the Mn(II) from its labile complexes may interfere with the MR signal generated as a result of SCA activation because the uncomplexed Mn(II) ion or its adduct with human serum albumin (HSA) has considerably higher relaxivity ($r_{1p}=7.92$ and $54.6 \text{ mM}^{-1}\text{s}^{-1}$ at 0.49 T and 25°C) than the majority of the monohydrated low molecular weight Mn(II) complexes (r_{1p} values are typically in the range of $2.0\text{-}5.4 \text{ mM}^{-1}\text{s}^{-1}$).^{27,29,31} In addition, Mn(II) has a PET isotope (^{52}Mn), which may offer a convenient way to follow the biodistribution of the agent during imaging as the local concentration of the complex can be determined by radioanalytical methods by using a cocktail of $^{52}\text{Mn}/^{55}\text{Mn}$ isotopic complexes.³² Furthermore, this isotopic mixture offers the possibility of combining PET (^{52}Mn) and MR (^{55}Mn) imaging modalities to provide anatomical and functional information.^{33,34}

In cancer diagnosis, mapping of tissue pH can potentially be used to recognize malignant processes at an early stage since the accelerated glucose metabolism of cancer cells results in a decrease of the extracellular and increase of the intracellular pH (Warburg effect).^{35,36} Several Gd(III)-based pH-sensitive SCA candidates were reported relying on the pH-dependent coordination of an ethylamine pendant arm.³⁷ In our previous study we have shown that the parent ligand PCTA can be successfully utilized as a platform in the design of Mn(II)-based alternatives to Gd(III).²⁹ By replacing one acetate arm in PCTA with an ethylamine pH-sensing moiety, we designed the heptadentate PC2A-EA chelator, which is expected to combine the advantageous metal binding properties of PCTA and the pH-responsive “on/off” coordination feature of the ethylamine pendant arm.^{38,39}



Scheme 1. Structure of the PC2A, PC2A-EA and PCTA ligands.

Protonation constants of the ligand were determined by pH-potentiometric titrations (0.15 M NaCl , 25°C). The log K values are listed in Table 1 along with the corresponding values previously determined for PC2A and PCTA (see ESI for additional data). The log K values reveal that substitution of an ethylamine group for an acetate in PCTA significantly changes the basicity as well as the protonation sequence of the ligand. This was also confirmed by ^1H

NMR titration performed in the pH range of 6–12 (Fig. S6 and S7 in the ESI).⁴⁰

Formation of PC2A-EA complexes with Mn(II) was studied by pH-potentiometry and ¹H relaxometry (Table 1). Considering the basicity of PC2A-EA (Table 1), it is not surprising that the stability constant of [Mn(PC2A-EA)] was found to be higher than those of the chelates formed with parent ligands.

Table 1. Protonation constants of the PC2A-EA, PC2A and PCTA ligands and stability constants of their Mn(II) complexes (25 °C, I=0.15 M NaCl).

	PC2A ^[b]	PC2A-EA	PCTA ^[d]
log K_1	12.25	11.34(1)	9.97
log K_2	5.97	8.93(2)	6.73
log K_3	3.47	6.91(3)	3.22
log K_4	1.99	1.97(3)	1.40
$\Sigma \log K_2^H$	18.22	18.25^[c]	16.70
log K_{MnL}	17.09	19.01(4)	16.83
log K_{MnL}^H	2.14	6.88(2)	1.96
log K_{MnHL}^H	–	2.50(3)	–
pMn ^[a]	8.64	9.27	9.74

[a] pMn = $-\log [Mn(II)_{free}]$, $c_{Mn} = c_L = 0.01$ mM; [b] Ref.³⁹ 25 °C, I=0.15 M NaCl; [c] the log K_2^H for the PC2A-EA is defined as the sum of log K_1^H and log K_3^H ; [d] Ref.³⁸, 25 °C, I=1.0 M KCl

The pMn values (pMn = $-\log [Mn(II)_{free}]$) for the [Mn(PC2A)], [Mn(PC2A-EA)] and [Mn(PCTA)][–] complexes were calculated by using the following conditions: $c_{Mn(II)} = c_{lig} = 0.01$ mM, pH=7.4, 25 °C (Table 1).³⁰ Under these conditions the pMn value obtained for [Mn(PC2A-EA)] (pMn=9.27) is the second highest value ever reported for a Mn(II) chelate, after the pMn of the non-hydrated [Mn(PCTA)][–] chelate.²⁹ This value appears to be higher than that of the [Mn(DOTA)]^{2–} complex (pMn=9.02), which means that less than the 0.01% of total Mn(II) chelated is expected to dissociate at pH=7.4 at equilibrium.

The formation of the Mn(II) complex was also monitored by following the T_1 relaxation times as a function of pH. The relaxivity vs. pH profile and the species distribution curves are shown in Figure 1. The relaxivity of [Mn(HPC2A-EA)]⁺ is very similar to those of monoaquated Mn(II) complexes and remains nearly constant (3.52 mM^{–1}s^{–1}) in the pH range of 3.7–5.8.⁴¹ This r_{1p} value suggests that q=1 for the protonated [Mn(HPC2A-EA)]⁺ complex. Below pH 3.5 r_{1p} increases owing to the formation of a diprotonated chelate followed by the dissociation of the complex. Raising the pH above 5.8 results in a noticeable decrease of r_{1p} , reaching a value of 2.07 mM^{–1}s^{–1} at pH 8.4 indicating the deprotonation and coordination of the ethylamine pendant to the Mn(II) ion resulting in the formation of a q=0 complex. This increase in r_{1p} relaxivity observed upon the protonation and decoordination of the amine moiety (as proved by ¹⁷O NMR) is more than 1.5 mM^{–1}s^{–1} unit in pure aqueous solutions while in human blood serum (tested by using commercialized Seronorm) the r_{2p} relaxivity changes even more notably ($\Delta r_{2p} = 6.6$ mM^{–1}s^{–1}).

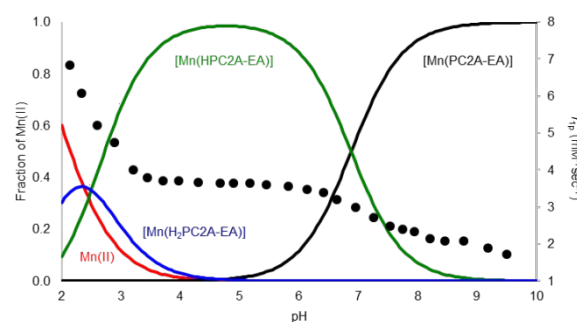


Figure 1. The species distribution curves calculated for the [Mn(PC2A-EA)] along with the pH dependence of its relaxivity (●) (I=0.15 M NaCl, T=25 °C, 0.49 T).

It is now accepted that the inertness of the complexes intended for *in vivo* applications as potential CAs is more important than their thermodynamic stability.^{1,42} The inertness of [Mn(HPC2A-EA)]⁺ was studied in reactions taking place between the complex and Cu(II) and Zn(II) ions acting as scavengers for the ligand (see ESI for more details). The transmetalation reactions were studied in the pH range of 2.2–3.4 under pseudo-first-order conditions by spectrophotometry (Cu(II)) and r_2 relaxometry (Zn(II)) at pH=6.0 as suggested by P. Caravan and coworkers.⁴³ As seen in Figure 2, the rate constants (k_{obs}) characterizing the transmetalation with Cu(II) increase with increasing [H⁺] showing “saturation” like behavior and they are independent of the Cu(II) concentration. This finding indicates that the dechelation of the complex occurs via the proton-assisted mechanism. The absence of positive intercept suggests that the spontaneous dissociation of the complex can be neglected.

Taking into account the concentration of different complex species as well as the protonation constants (K_H) of [Mn(HPC2A-EA)] ($K_H = [Mn(H_2PC2A-EA)]/[Mn(HPC2A-EA)] \cdot [H^+]$) the rate equation can be given as follows:

$$k_{obs} = \frac{k_1[H^+]}{1 + K_H[H^+]} \quad (1)$$

where k_1 is the rate constant characterizing the proton-assisted dissociation. The value of k_1 and K_H were found to be 0.6 ± 0.01 M^{–1}s^{–1} and 102 ± 5 M^{–1}, respectively. The k_1 is an order of magnitude lower than the value determined for the [Mn(1,4-DO2AM^{Me2})]²⁺ complex²⁸ and just one order of magnitude higher than that of [Mn(DOTA)]^{2–}, which are the most inert monoquated and nonaquated Mn(II) chelates, respectively. Kinetic inertness of [Mn(HPC2A-EA)]⁺ was also evaluated by using the protocol suggested by P. Caravan and coworkers.⁴³ The pseudo-first-order rate constant was found to be $(3.54 \pm 0.04) \times 10^{-6}$ s^{–1} ($t_{1/2} = 54.4$ h) whereas under the same conditions [Mn(PyC3A)(H₂O)][–] (a compound suggested recently as CA candidate) dissociates with the rate of 6.76×10^{-4} s^{–1} (corresponding to $t_{1/2} = 0.285$ h) i.e. the [Mn(HPC2A-EA)(H₂O)]⁺ is 190 times more inert than the given reference compound.⁴³

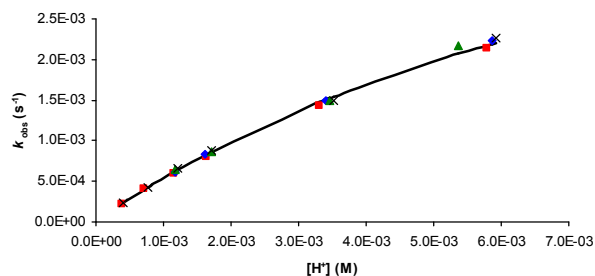


Figure 2. Dependence of the pseudo-first-order rate constants (k_{obs}) on the concentration of H^+ and Cu(II) ions for the $[\text{Mn}(\text{HPC2A-EA})]$ complex. The excess of the exchanging metal ion was 10 (■), 20 (●), 30 (▲) and 40 (×) folds. The lines correspond to the best fit of the k_{obs} values to the Eqn. 1.

An important part of the characterization of a potential MRI CA is the determination of the parameters governing its relaxivity such as exchange rate of the bound (q) water molecule (k_{ex}). The presence of an inner sphere water molecule was confirmed by using the method proposed by Gale et al.⁴⁴ while its exchange rate was determined by measuring the transversal ^{17}O relaxation rates ($1/T_2$) at different temperatures.⁴⁵ The k_{ex} ($(4.0 \pm 0.2) \times 10^7 \text{ s}^{-1}$) is nearly an order of magnitude lower than that of $[\text{Mn}(\text{EDTA})]^{2-}$ ($k_{\text{ex}}^{298} = 47.1 \times 10^7 \text{ s}^{-1}$) and approximately $1/4^{\text{th}}$ of that determined for $[\text{Mn}(\text{PC2A})(\text{H}_2\text{O})]$ ($k_{\text{ex}}^{298} = 15.2 \times 10^7 \text{ s}^{-1}$). These differences can be rationalized by considering the structures of these complexes: the open-chain $[\text{Mn}(\text{EDTA})]^{2-}$ has a flexible structure facilitating the water exchange while $[\text{Mn}(\text{HPC2A-EA})(\text{H}_2\text{O})]^+$ has a more compact coordination cage than $[\text{Mn}(\text{PC2A})(\text{H}_2\text{O})]$ resulting in a slower water exchange rate (see ESI for more details).

The efficacy of the $[\text{Mn}(\text{PC2A-EA})]$ complex as pH-sensitive MRI probe was also evaluated in MR imaging experiments at 1, 1.5 and 3 T magnetic field strength (to have an idea about the field dependency of relaxivity at high fields). Phantom MR images of 1.0 mM complex solution at different pH values were recorded at 3 T in Seronorm (Seronorm = lyophilized human blood serum with no preservatives or stabilizers added) redissolved in distilled water are shown in Figure 3. (see ESI for more data). Analysis of the MR images indicate that the signal intensity of the samples depend on their pH (both T_1 and T_2 weighted images, but the latter being more pronounced) thereby confirming that even these small changes in relaxation times can be followed and visualized by using commercialized MRI scanners (some estimations on what signal change might be expected in vivo are included in ESI).

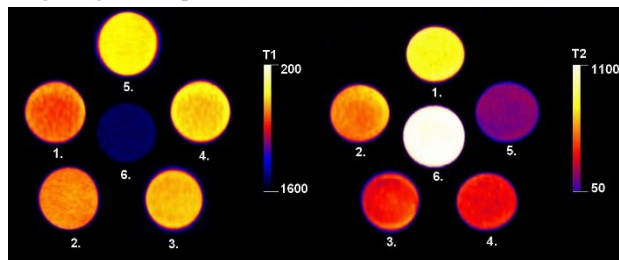


Figure 3. Representative T_1 - (left) and T_2 - weighted (right) MRI images (3 T) of the $[\text{Mn}(\text{PC2A-EA})]$ complex in human serum (Seronorm) at different pH values (pH=7.50 (1), 7.25 (2), 7.08 (3), 6.81 (4) and 6.67 (5), $c_{[\text{Mn}(\text{PC2A-EA})]} = 1 \text{ mM}$). The T_1 relaxation times of the samples are: 298 ± 2 (1), 257 ± 2 (2), 232 ± 2 (3), 233 ± 2 (4), 222 ± 2 (5) ms, while the T_2 data are as follows 456 ± 52 (1), 200 ± 11 (2), 144 ± 6 (3), 125 ± 5 (4) and 113 ± 4 (5) ms

(TRs=3500 ms, TE=7.45 msec, spatial resolution=0.481x0.417x1 mm³).

In conclusion, we have demonstrated that $[\text{Mn}(\text{PCTA})]^-$ can be converted to a pH-sensitive MRI CA candidate by substituting an ethylamine moiety for one of the acetate sidearms of PCTA. A decrease in pH results in the protonation and decoordination of the ethylamine moiety, followed by the coordination of an inner sphere water molecule. The r_{1p} relaxivity of $[\text{Mn}(\text{PC2A-EA})]$ increased from 2.04 at pH 8.4 to $3.54 \text{ mM}^{-1}\text{s}^{-1}$ at pH 6.0 (0.49 T, 25 °C) due to the appearance of the metal bound water molecule (these changes are being even more pronounced in T_2 “dimension” in Seronorm solutions as the r_{2p} was found to change from 1.71 (pH=7.5) to 8.34 (pH=6.67) $\text{mM}^{-1}\text{s}^{-1}$ at 3 T). pH-potentiometric studies revealed that the protonation constant of the complex ($\log K_{\text{MnL}}^{\text{H}} = 6.88(2)$) is nearly optimal for detecting pH changes in the physiologically relevant pH range. Thermodynamic and kinetic measurements showed that the thermodynamic stability ($\text{pMn} = 9.27$) and kinetic inertness ($t_{1/2} = 8 \times 10^3 \text{ h}$ at pH=7.4) of $[\text{Mn}(\text{PC2A-EA})]$ is among the highest reported for a monohydrated Mn(II) complex. The water exchange rate was found to be relatively slow ($k_{\text{ex}} = 4.0 \pm 0.2 \times 10^7 \text{ s}^{-1}$) by variable temperature ^{17}O NMR. In summary, the favorable kinetic and relaxometric properties of $[\text{Mn}(\text{PC2A-EA})]$ make this complex a promising Mn(II)-based pH-responsive CA candidate.

ASSOCIATED CONTENT

Supporting Information

Details of the synthesis, descriptions of the thermodynamic, kinetic, ^1H relaxometric, ^{17}O NMR relaxation and phantom MRI experiments (PDF).

AUTHOR INFORMATION

Corresponding Author

kalman.ferenc@science.unideb.hu
gyula.tircso@science.unideb.hu

Notes

The authors declare no competing financial interests.

ACKNOWLEDGMENT

The authors thank Dr. Zoltan Kovacs (UTSW) for helpful discussions. The financial support arriving from the Hungarian National Research, Development and Innovation Office (NKFIH K-120224 project) and the János Bolyai Research Scholarship of the Hungarian Academy of Sciences (G.T. and F.K.K.) are also thanked. The research was supported by the ÚNKP-18-4 new national excellence program of the Ministry of Human Capacities (G.T. and F.K.K.) and by the EU and co-financed by the European Regional Development Fund under the project GINOP-2.3.2-15-2016-00008.

REFERENCES

- (1) The Chemistry of Contrast Agents in Medical Magnetic Resonance Imaging: Helm/The Chemistry of Contrast Agents in Medical Magnetic Resonance Imaging; Merbach, A., Helm, L., Tóth, É., Eds.; John Wiley & Sons, Ltd: Chichester, UK, 2013.
- (2) Jacques, V.; Desreux, J. F. New Classes of MRI Contrast Agents. In Contrast Agents I; Krause, W., Ed.; de Meijere, A., Kessler, H., Ley, S. V., Thiem, J., Vögtle, F., Houk, K. N., Lehn, J.-M., Schreiber, S. L., Trost, B. M., Yamamoto, H., Series Eds.; Springer Berlin Heidelberg: Berlin, Heidelberg, 2002; Vol. 221, pp 123–164.
- (3) Bonnet, C. S.; Tóth, É. Smart Contrast Agents for Magnetic Resonance Imaging. *Chim. Int. J. Chem.* **2016**, 70 (1), 102–108.

- (4) Zhang, L.; Martins, A. F.; Zhao, P.; Wu, Y.; Tircsó, G.; Sherry, A. D. Lanthanide-Based $T_{2\text{ex}}$ and CEST Complexes Provide Insights into the Design of PH Sensitive MRI Agents. *Angew. Chem. Int. Ed.* **2017**, 56 (52), 16626–16630.
- (5) Kenwright, A. M.; Kuprov, I.; De Luca, E.; Parker, D.; Pandya, S. U.; Senanayake, P. K.; Smith, D. G. 19F NMR Based PH Probes: Lanthanide(III) Complexes with PH-Sensitive Chemical Shifts. *Chem. Commun.* **2008**, No. 22, 2514.
- (6) Kálmán, F. K.; Woods, M.; Caravan, P.; Jurek, P.; Spiller, M.; Tircsó, G.; Király, R.; Brücher, E.; Sherry, A. D. Potentiometric and Relaxometric Properties of a Gadolinium-Based MRI Contrast Agent for Sensing Tissue PH. *Inorg. Chem.* **2007**, 46 (13), 5260–5270.
- (7) Ratnakar, S. J.; Viswanathan, S.; Kovacs, Z.; Jindal, A. K.; Green, K. N.; Sherry, A. D. Europium(III) DOTA-Tetraamide Complexes as Redox-Active MRI Sensors. *J. Am. Chem. Soc.* **2012**, 134 (13), 5798–5800.
- (8) Do, Q. N.; Ratnakar, J. S.; Kovács, Z.; Sherry, A. D. Redox- and Hypoxia-Responsive MRI Contrast Agents. *ChemMedChem* **2014**, 9 (6), 1116–1129.
- (9) Loving, G. S.; Mukherjee, S.; Caravan, P. Redox-Activated Manganese-Based MR Contrast Agent. *J. Am. Chem. Soc.* **2013**, 135 (12), 4620–4623.
- (10) Fossheim, S. L.; Il'yasov, K. A.; Hennig, J.; Bjørnerud, A. Thermosensitive Paramagnetic Liposomes for Temperature Control during MR Imaging-Guided Hyperthermia: In Vitro Feasibility Studies. *Acad. Radiol.* **2000**, 7 (12), 1107–1115.
- (11) Terreno, E.; Delli Castelli, D.; Cabella, C.; Dastrù, W.; Sanino, A.; Stancanello, J.; Tei, L.; Aime, S. Paramagnetic Liposomes as Innovative Contrast Agents for Magnetic Resonance (MR) Molecular Imaging Applications. *Chem. Biodivers.* **2008**, 5 (10), 1901–1912.
- (12) Yeo, S. Y.; de Smet, M.; Langereis, S.; Vander Elst, L.; Muller, R. N.; Grüll, H. Temperature-Sensitive Paramagnetic Liposomes for Image-Guided Drug Delivery: Mn^{2+} versus $[\text{Gd}(\text{HPDO3A})(\text{H}_2\text{O})]$. *Biochim. Biophys. Acta BBA - Biomembr.* **2014**, 1838 (11), 2807–2816.
- (13) Rudin, M. Target Watching with a Beady Eye. *Nat. Biotechnol.* **2000**, 18 (4), 383–383.
- (14) Napolitano, R.; Pariani, G.; Fedeli, F.; Baranyai, Z.; Aswendt, M.; Aime, S.; Gianolio, E. Synthesis and Relaxometric Characterization of a MRI Gd-Based Probe Responsive to Glutamic Acid Decarboxylase Enzymatic Activity. *J. Med. Chem.* **2013**, 56 (6), 2466–2477.
- (15) Hingorani, D. V.; Randtke, E. A.; Pagel, M. D. A CatalyCEST MRI Contrast Agent That Detects the Enzyme-Catalyzed Creation of a Covalent Bond. *J. Am. Chem. Soc.* **2013**, 135 (17), 6396–6398.
- (16) Gündüz, S.; Vibhute, S.; Botár, R.; Kálmán, F. K.; Tóth, I.; Tircsó, G.; Regueiro-Figueroa, M.; Esteban-Gómez, D.; Platas-Iglesias, C.; Angelovski, G. Coordination Properties of GdDO3A-Based Model Compounds of Bioresponsive MRI Contrast Agents. *Inorg. Chem.* **2018**, 57 (10), 5973–5986.
- (17) Regueiro-Figueroa, M.; Gündüz, S.; Patinec, V.; Logothetis, N. K.; Esteban-Gómez, D.; Tripiet, R.; Angelovski, G.; Platas-Iglesias, C. Gd³⁺-Based Magnetic Resonance Imaging Contrast Agent Responsive to Zn²⁺. *Inorg. Chem.* **2015**, 54 (21), 10342–10350.
- (18) Aime, S.; Botta, M.; Gianolio, E.; Terreno, E. Ap(O2)-Responsive MRI Contrast Agent Based on the Redox Switch of Manganese(II/III) - Porphyrin Complexes. *Angew. Chem. Int. Ed.* **2000**, 39 (4), 747–750.
- (19) Di Gregorio, E.; Ferrauto, G.; Gianolio, E.; Lanzardo, S.; Carrera, C.; Fedeli, F.; Aime, S. An MRI Method To Map Tumor Hypoxia Using Red Blood Cells Loaded with a PO₂-Responsive Gd-Agent. *ACS Nano* **2015**, 9 (8), 8239–8248.
- (20) Rojas-Quijano, F. A.; Tircsó, G.; Tircsóné Benyó, E.; Baranyai, Z.; Tran Hoang, H.; Kálmán, F. K.; Gulaka, P. K.; Kodibagkar, V. D.; Aime, S.; Kovács, Z.; et al. Synthesis and Characterization of a Hypoxia-Sensitive MRI Probe. *Chem. - Eur. J.* **2012**, 18 (31), 9669–9676.
- (21) Takács, A.; Napolitano, R.; Purgel, M.; Bényei, A. C.; Zékány, L.; Brücher, E.; Tóth, I.; Baranyai, Z.; Aime, S. Solution Structures, Stabilities, Kinetics, and Dynamics of DO3A and DO3A-Sulphonamide Complexes. *Inorg. Chem.* **2014**, 53 (6), 2858–2872.
- (22) Grobner, T. Gadolinium – a Specific Trigger for the Development of Nephrogenic Fibrosing Dermopathy and Nephrogenic Systemic Fibrosis? *Nephrol. Dial. Transplant.* **2006**, 21 (4), 1104–1108.
- (23) Darrah, T. H.; Prutsman-Pfeiffer, J. J.; Poreda, R. J.; Ellen Campbell, M.; Hauschka, P. V.; Hannigan, R. E. Incorporation of Excess Gadolinium into Human Bone from Medical Contrast Agents. *Metallomics* **2009**, 1 (6), 479.
- (24) Walter, E.; Ashley, S.; Livingstone, C.; Kemp, I.; Alsaffar, S. Manganese Elimination in Hepatobiliary Failure. *J. Intensive Care Soc.* **2016**, 17 (4), 360–361.
- (25) Erstad, D. J.; Ramsay, I. A.; Jordan, V. C.; Sojoodi, M.; Fuchs, B. C.; Tanabe, K. K.; Caravan, P.; Gale, E. M. Tumor Contrast Enhancement and Whole-Body Elimination of the Manganese-Based Magnetic Resonance Imaging Contrast Agent Mn-PyC3A: *Invest. Radiol.* **2019**, 54 (11), 697–703.
- (26) Gale, E. M.; Wey, H.-Y.; Ramsay, I.; Yen, Y.-F.; Sosnovik, D. E.; Caravan, P. A Manganese-Based Alternative to Gadolinium: Contrast-Enhanced MR Angiography, Excretion, Pharmacokinetics, and Metabolism. *Radiology* **2018**, 286 (3), 865–872.
- (27) Drahoš, B.; Lukeš, I.; Tóth, É. Manganese(II) Complexes as Potential Contrast Agents for MRI. *Eur. J. Inorg. Chem.* **2012**, 2012 (12), 1975–1986.
- (28) Forgács, A.; Tei, L.; Baranyai, Z.; Tóth, I.; Zékány, L.; Botta, M. A Bisamide Derivative of $[\text{Mn}(\text{1,4-DO2A})]$ - Solution Thermodynamic, Kinetic, and NMR Relaxometric Studies. *Eur. J. Inorg. Chem.* **2016**, 2016 (8), 1165–1174.
- (29) Garda, Z.; Molnár, E.; Kálmán, F. K.; Botár, R.; Nagy, V.; Baranyai, Z.; Brücher, E.; Kovács, Z.; Tóth, I.; Tircsó, G. Effect of the Nature of Donor Atoms on the Thermodynamic, Kinetic and Relaxation Properties of Mn(II) Complexes Formed With Some Trisubstituted 12-Membered Macrocyclic Ligands. *Front. Chem.* **2018**, 6, 232.
- (30) Drahoš, B.; Kotek, J.; Hermann, P.; Lukeš, I.; Tóth, É. Mn²⁺ Complexes with Pyridine-Containing 15-Membered Macrocycles: Thermodynamic, Kinetic, Crystallographic, and ¹H/¹⁷O Relaxation Studies. *Inorg. Chem.* **2010**, 49 (7), 3224–3238.
- (31) Kálmán, F. K.; Tircsó, G. Kinetic Inertness of the Mn²⁺ Complexes Formed with AAZTA and Some Open-Chain EDTA Derivatives. *Inorg. Chem.* **2012**, 51 (19), 10065–10067.
- (32) Malikidogo, K. P.; Da Silva, I.; Morfin, J.-F.; Lacerda, S.; Barantin, L.; Sauvage, T.; Sobilo, J.; Lerondel, S.; Tóth, É.; Bonnet, C. S. A Cocktail of ¹⁶⁵Er(III) and Gd(III) Complexes for Quantitative Detection of Zinc Using SPECT and MRI. *Chem. Commun.* **2018**, 54 (55), 7597–7600.
- (33) Graves, S. A.; Hernandez, R.; Fonslet, J.; England, C. G.; Valdovinos, H. F.; Ellison, P. A.; Barnhart, T. E.; Elema, D. R.; Theuer, C. P.; Cai, W.; et al. Novel Preparation Methods of ⁵²Mn for ImmunoPET Imaging. *Bioconjug. Chem.* **2015**, 26 (10), 2118–2124.
- (34) Vitor, T.; Martins, K. M.; Ionescu, T. M.; Cunha, M. L. da; Baroni, R. H.; Garcia, M. R. T.; Wagner, J.; Campos Neto, G. de C.; Nogueira, S. A.; Guerra, E. G.; et al. PET/MRI: A Novel Hybrid Imaging Technique. Major Clinical Indications and Preliminary Experience in Brazil. *Einstein São Paulo* **2017**, 15 (1), 115–118.
- (35) De Leon-Rodriguez, L. M.; Lubag, A. J. M.; Malloy, C. R.; Martinez, G. V.; Gillies, R. J.; Sherry, A. D. Responsive MRI Agents for Sensing Metabolism in Vivo. *Acc. Chem. Res.* **2009**, 42 (7), 948–957.
- (36) Swietach, P.; Vaughan-Jones, R. D.; Harris, A. L.; Hulikova, A. The Chemistry, Physiology and Pathology of PH in Cancer. *Philos. Trans. R. Soc. B Biol. Sci.* **2014**, 369 (1638), 20130099–20130099.
- (37) Baranyai, Z.; Rolla, G. A.; Negri, R.; Forgács, A.; Giovenzana, G. B.; Tei, L. Comprehensive Evaluation of the Physicochemical Properties of Ln^{III} Complexes of Aminoethyl-DO3A as PH-Responsive T₁-MRI Contrast Agents. *Chem. - Eur. J.* **2014**, 20 (10), 2933–2944.
- (38) Tircsó, G.; Kovács, Z.; Sherry, A. D. Equilibrium and

1 Formation/Dissociation Kinetics of Some Ln^{III} PCTA
2 Complexes. *Inorg. Chem.* **2006**, 45 (23), 9269–9280.
3 (39) Nagy, V.; Póta, K.; Garda, Z.; Barriada, J. L.; Tripier, R.; Platas-
4 Iglesias, C.; Tóth, É.; Tircsó, G. manuscript in preparation.
5 (40) Aime, S.; Botta, M.; Geninatti Crich, S.; Giovenzana, G. B.;
6 Jommi, G.; Pagliarin, R.; Sisti, M. Synthesis and NMR Studies of
7 Three Pyridine-Containing Triaza Macrocyclic Triacetate
8 Ligands and Their Complexes with Lanthanide Ions. *Inorg.*
9 *Chem.* **1997**, 36 (14), 2992–3000.
10 (41) Pota, K.; Garda, Z.; Kálmán, F. K.; Barriada, J. L.; Esteban-
11 Gómez, D.; Platas-Iglesias, C.; Tóth, I.; Brücher, E.; Tircsó, G.
12 Taking the next Step toward Inert Mn²⁺ Complexes of Open-
13 Chain Ligands: The Case of the Rigid PhDTA Ligand. *New J.*
14 *Chem.* **2018**, 42 (10), 8001–8011.
15 (42) Baranyai, Z.; Brücher, E.; Uggeri, F.; Maiocchi, A.; Tóth, I.;
16 András, M.; Gáspár, A.; Zékány, L.; Aime, S. The Role of
17 Equilibrium and Kinetic Properties in the Dissociation of
18 Gd[DTPA-Bis(Methylamide)] (Omniscan) at near to
19 Physiological Conditions. *Chem. - Eur. J.* **2015**, 21 (12), 4789–
20 4799.
21 (43) Gale, E. M.; Atanasova, I. P.; Blasi, F.; Ay, I.; Caravan, P. A
22 Manganese Alternative to Gadolinium for MRI Contrast. *J. Am.*
23 *Chem. Soc.* **2015**, 137 (49), 15548–15557.
24 (44) Gale, E. M.; Zhu, J.; Caravan, P. Direct Measurement of the
25 Mn(II) Hydration State in Metal Complexes and Metalloproteins
26 through ¹⁷O NMR Line Widths. *J. Am. Chem. Soc.* **2013**, 135
27 (49), 18600–18608.
28 (45) Swift, T. J.; Connick, R. E. Erratum: NMR-Relaxation
29 Mechanisms of ¹⁷O in Aqueous Solutions of Paramagnetic
30 Cations and the Lifetime of Water Molecules in the First
31 Coordination Sphere. *J. Chem. Phys.* **1964**, 41 (8), 2553–2554.

